Phase sensitivity of a nonlinear Bragg grating response under bidirectional illumination

Article *in* Journal of the Optical Society of America B · May 1999

DOI: 10.1364/JOSAB.16.000774

2 authors:

Yury Logvin
ArtIC Photonics, Ottawa, Canada
85 PUBLICATIONS **937** CITATIONS
SEE PROFILE

V. M. Volkov
Belarusian State University
72 PUBLICATIONS **224** CITATIONS
SEE PROFILE

Phase sensitivity of a nonlinear Bragg grating response under bidirectional illumination

Yu. A. Logvin

Institute of Physics, Belarus Academy of Sciences, Skaryna Avenue 70, Minsk 220072, Belarus

V. M. Volkov

Institute of Mathematics, Belarus Academy of Sciences, Surganov Street 11, Minsk 220072, Belarus

Received September 3, 1998; revised manuscript received December 14, 1998

The response of a nonlinear Bragg grating under bidirectional illumination is studied. By analytical and numerical techniques it is found that the threshold for bistability, pulsation development, and spatial transverse instability is strongly influenced by the phase difference between fields incident from opposite directions. Breakup of pulsations that are symmetrical for both directions into nonsymmetrical pulsations is demonstrated. Solutions for focusing and defocusing nonlinearities are found to be related by means of changes in phase of the incident wave. A change of phase of π may lead to the emergence of a regular spatiotemporal light structure or may cause a transverse static pattern to become turbulent. © 1999 Optical Society of America [S0740-3224(99)00405-1]

OCIS codes: 050.2770, 190.1450, 190.3100.

1. INTRODUCTION

There has been significant progress in recent years in experimental studies of the gap-soliton formation and switching processes in nonlinear Bragg gratings (NBG's).[1–5] In contrast to the materials used in earlier experiments,[6–8] a uniform fiber Bragg grating was used by Eggleton *et al.* to demonstrate the generation of the Bragg grating soliton[1] and the formation of trains of solitons[2] owing to modulational instability in the grating. Observation of quasi-cw nonlinear switching and multiple gap-soliton formation within the bandgap of a NBG was reported by Taverner *et al.*,[3] who also realized an all-optical AND gate based on coupled gap-soliton formation in a fiber Bragg grating.[4]

A theoretical background for the recent experiments was created much earlier in the research in which on the one hand a cw regime of interaction of light with a NBG[9–12] was consider and on the other hand localized solutions for light excitation (solitons) inside the grating were sought.[13–16] (For an overview, see Ref. 17.)

In spite of the fact that the theory of light propagation in NBG's is rather well elaborated, the case of bidirectional illumination of NBG has not received much attention compared with the case of unidirectional illumination. Here we aim to fill this gap, at least partly. Concentrating on the case of exact Bragg resonance, we show here by means of analytical and numerical techniques that the phase difference between light fields illuminating a NBG simultaneously from both sides is an important parameter in determining the NBG response. It should be noted that previously the phase effects in NBG's were considered in the context of chirped or phase-shifted structures (see, e.g., Ref. 18 and references therein), where a nonuniform variation of the phase of the grating was assumed. In the present paper attention is paid to the influence of the phase of an electric field on the boundary of a grating at the threshold of instability. The problem of bidirectional illumination of the NBG is not only of interest from a theoretical point of view but may also be important for possible applications in which one light beam is controlled with another. (Note that recently the method of excitation of two-color gap solitons in a Bragg grating with quadratic nonlinearity by counterpropagating pulses was suggested.[19])

We start our study with the case of unidirectional illumination and assume that the second incident beam is negligibly weak compared with the basic beam. Depending on the phase difference between the fields (i.e., whether the incident fields are in phase or out of phase), the bistability threshold is changed significantly.

Further, we consider the case of equal intensities of beams illuminating the grating from both sides. We find that changing the phase difference (e.g., from zero to π) enables us to excite a gap soliton in the structure or to modify the regime of transmission (reflection) from self-pulsating to static. We demonstrate an example of symmetry-breaking bifurcation in the NBG. The relationship of the properties of the NBG for focusing and defocusing nonlinearities is also discussed.

Finally, we take into account the transverse degree of freedom and numerically investigate transverse pattern formation in the grating. Here, in contrast to the case of a purely Kerr medium without a grating,[20] the phase parameter is an important factor in determining the threshold for pattern formation as well as the pattern dynamics.

2. BASIC EQUATIONS

In the framework of coupled-mode theory,[9,21] two counterpropagating waves in a nonlinear Bragg grating are described by the following set of equations:

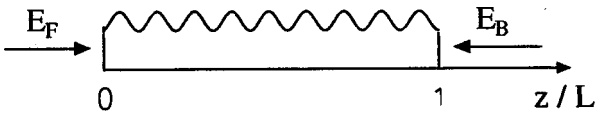

Fig. 1. Nonlinear Bragg grating of length L illuminated from opposite sides by light waves E_F and E_B.

$$\frac{\partial E_F}{\partial z} + \frac{n_0}{c}\frac{\partial E_F}{\partial t} = i\kappa E_B \exp(-i2\delta z) + i\gamma(|E_F|^2 + 2|E_B|^2)E_F, \quad (1)$$

$$\frac{\partial E_B}{\partial z} - \frac{n_0}{c}\frac{\partial E_B}{\partial t} = -i\kappa E_F \exp(i2\delta z) - i\gamma(|E_B|^2 + 2|E_F|^2)E_B, \quad (2)$$

where E_F (E_B) is the normalized slowly varying envelope of the forward (backward) wave, c/n_0 is the group velocity of the waves, κ is a coefficient that describes the strength of linear coupling, δ is a detuning parameter, and γ is a nonlinear phase-modulation coefficient. The boundary conditions

$$E_F(z = 0, t) = F_0, \qquad E_B(z = L, t) = B_0 \exp(i\theta) \quad (3)$$

correspond to illumination of a NGB of length L simultaneously from the left and from the right by light fields with intensities $|F_0|^2$ and $|B_0|^2$, respectively, with a phase difference θ between them (see Fig. 1).

Introducing $E_F = F\exp(i\phi_F)$ and $E_B = B\exp(i\phi_B)$, we can find time-independent solutions as outlined in Ref. 9. The constants of motion

$$C_1 = F^2 - B^2, \quad (4)$$

$$C_2 = 2\kappa LFB\cos\psi + 2\delta LF^2 + 3\gamma LF^2B^2, \quad (5)$$

where $\psi = \phi_B - \phi_F - 2\delta z$, enable us to get an equation for the forward flux $I_F = F^2$:

$$\left(\frac{L}{2}\frac{dI_F}{dz}\right)^2 = (\kappa L)^2 I_F(I_F - C_1) - [C_2/2 - \delta L I_F - I_F(I_F - C_1)]^2. \quad (6)$$

Unidirectional illumination implies that $C_2 = 0$ and $C_1 \neq 0$. The opposite case, $C_2 \neq 0$ and $C_1 = 0$, corresponds to illumination of the NBG by light of equal intensity from both sides. Finding four zeros of the polynomial on the right-hand side of Eq. (6) [$I_1 > I_F(z) > I_2 > I_3 > I_4$] permits us to obtain an analytical solution of the problem in terms of Jacobian integrals.[22]

3. WEAK BACKWARD WAVE

We consider first the case when the signal incident upon the grating from the right is a small part of the basic signal that is incident from the left. The curves in Fig. 2 show the intensity of the light transmitted to the right $I_T = I_F(z = L)$ for three cases. The solid curve shows the well-known result of bistable characteristics for unidirectional illumination,[9] whereas the two dashed curves correspond to cases when the grating is illuminated from the right by a light wave of low intensity ($I_B = 0.01$), with the difference that phase θ for curve (a) is π and that phase θ for curve (c) is zero. (Note that the parameters chosen and the scaling correspond to those used by Winful *et al.*[9–11])

From a comparison of the curves in Fig. 2 one can see the strong sensitivity of the NBG response to a small additional amount of illumination from the right. This proves that with a light wave with intensity 0.01 one can control the intensity threshold ($I_{th} \sim 2$) for switching the transmittivity to the upper state within an accuracy of ~10%. The most important parameter for this control is the phase difference θ. If the fields incident upon the grating are out of phase, the switching threshold is reduced, whereas for the in-phase fields this threshold becomes higher.

It is interesting also to compare spatiotemporal dynamics for the three cases on the upper branch, where the steady-state solution is known to be modulationally unstable.[10,11] [We have numerically integrated Eqs. (1) and (2) and achieved the same results with both explicit and implicit difference schemes.] Figure 3 shows the corresponding transmitted (to the right) and reflected pulsations after they have settled after some transient processes for the intensity values denoted by the arrows in Fig. 2. The regime illustrated in Fig. 3(a) may be referred to as a plain T-period regime, whereas Figs. 3(b) and 3(c) show 2T- and 3T-periodic pulsations, respectively. We have found that these periodic regimes are robust within the broad interval of the intensity of the forward beam (I_0 from 2.1 to 2.3) of the corresponding curve in Fig. 2, so the change in the phase of the weak backward field is responsible for the change of the regimes. In accordance with the results of Ref. 10, we have observed emergence of nonregular pulsations for increased incident intensity I_0 (e.g., $I_0 > 2.3$ for curve c of Fig. 2).

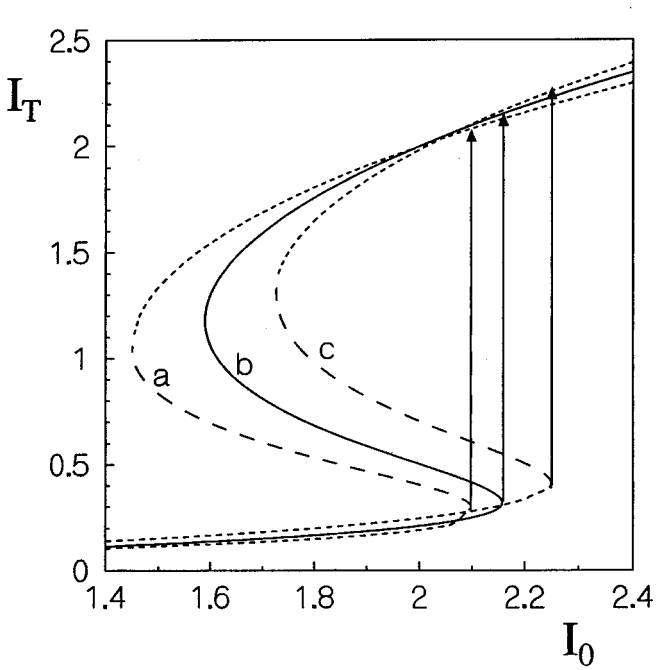

Fig. 2. Light intensity transmitted to the right I_T versus intensity incident from the left I_0 at $\kappa L = 2$, $\gamma L = 2/3$, $\delta = 0$ and parameters of the wave incident from the right: a, $I_B = 0.01$, $\theta = \pi$; b, $I_B = 0.0$; c, $I_B = 0.01$, $\theta = 0$.

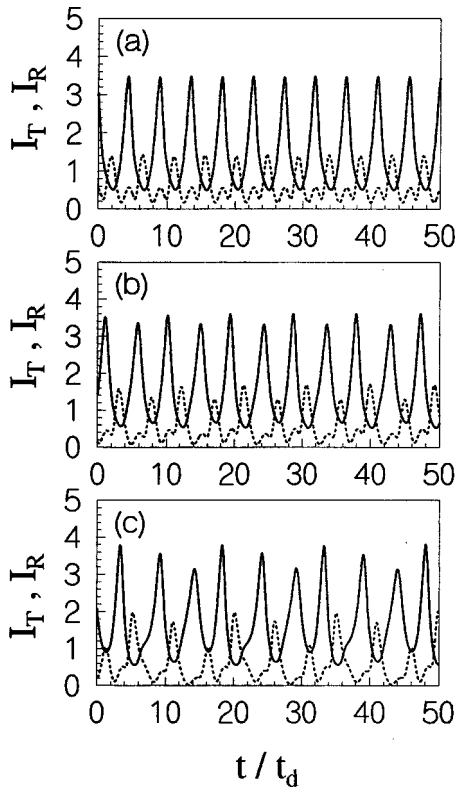

Fig. 3. Intensity pulsations for waves transmitted through grating I_T (solid curves) and reflected from grating I_R (dashed curves) from the cases a–c depicted by the corresponding arrows in Fig. 2.

The sequence of period-adding bifurcations such as that shown in Fig. 3 is well known in bistable optical systems with external feedback.[23,24] This sequence has also been found in a nonlinear distributed-feedback system consisting of thin films of an optically resonant medium separated by linear layers.[25] In those cases a period of pulsations was associated with circulation of light within the feedback loop. For the pulsations in Fig. 3 the period is significantly larger than $t_d = Ln_0/c$, which can be explained by the fact that the group velocity of the light in the grating vanishes inside the bandgap. However, for light beams of higher intensity the period of pulsation may be equal to or even less than $t_d = Ln_0/c$, as we shall see below.

4. EQUAL INTENSITIES FROM BOTH SIDES

Let us consider now the case of equal intensities of beams illuminating the NBG from both sides. Changing the parameter C_2, we obtain the characteristics presented in Fig. 4. Here, in Fig. 4(a) the light intensity in the center of the grating $I(z = L/2)$ is plotted versus incident intensity I_0. The solid curve corresponds to the in-phase incident waves ($\theta = 0$), and the dashed curve corresponds to the out-of-phase incident waves ($\theta = \pi$). The intensity distribution inside the grating for incident intensity $I_0 = 1.5$ is shown in Fig. 5(a). It can be seen that in the center of the NBG there is a minimum of intensity for $\theta = 0$ and a maximum of intensity for $\theta = \pi$.

Note that to obtain these curves we should use different solutions of Eq. (6); i.e., for the case of $\theta = 0$ we should start integration with the I_2 root of the polynomial, and the explicit form of the solution is

$$I(z/L) = \frac{I_2(I_1 - I_3) + I_3(I_1 - I_2)\mathrm{sn}^2[(z - 0.5)\sigma/L, m]}{I_1 - I_3 + (I_1 - I_2)\mathrm{sn}^2[(z - 0.5)\sigma/L, m]}, \tag{7}$$

where $\sigma = [(I_1 - I_3)(I_2 - I_4)]^{1/2}$, $m = (I_1 - I_2)(I_3 - I_4)/(I_1 - I_3)(I_2 - I_4)$, and sn is a Jacobian elliptical function, whereas the dashed curve is given by

$$I(z/L) = \frac{I_1(I_2 - I_4) + I_4(I_1 - I_2)\mathrm{sn}^2[(0.5 - z)\sigma/L, m]}{I_2 - I_4 + (I_1 - I_2)\mathrm{sn}^2[(0.5 - z)\sigma/L, m]}, \tag{8}$$

where the maximal root I_1 is taken as a starting point for integration.[22]

To gain an insight into the response of the grating at arbitrary phase θ we present Figs. 5(b) and 5(c), which correspond to $\theta = \pi/3$ and $\theta = 2\pi/3$, respectively. As θ increases from zero, distributions for F^2 and B^2 no longer coincide [as they do in Fig. 5(a)], but they differ by the constant C_1 according to Eq. (5). The curves in Fig. 5(b) show that the intensities decay from the boundaries down the grating. Note also that at equal incident intensities the output intensity is higher for the backward wave. At $\theta \sim \pi/2$ the response of the structure is changed abruptly, and the curves take the form shown in Fig. 5(c). Here, unlike in Fig. 5(b), the maxima of the intensities lie close to the center of the structure, and the output is greater for the forward wave. Approaching $\theta = \pi$, we get distributions $F^2 = B^2$ shown by the dashed curve in

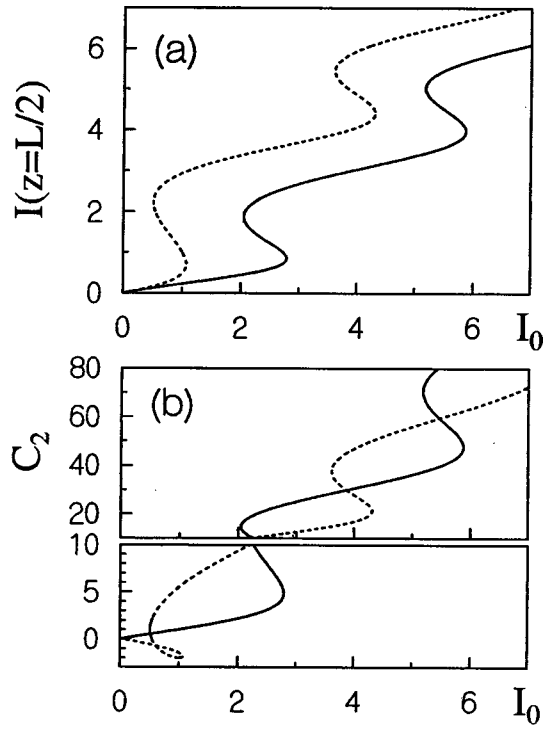

Fig. 4. (a) Light intensity in the middle of the grating and (b) constant C_2 versus the input intensity at equal amplitudes of incident waves at $\kappa L = 2$, $\gamma L = 2/3$, $\delta = 0$. Solid (dashed) curves correspond to in-phase (out-of-phase) incident waves.

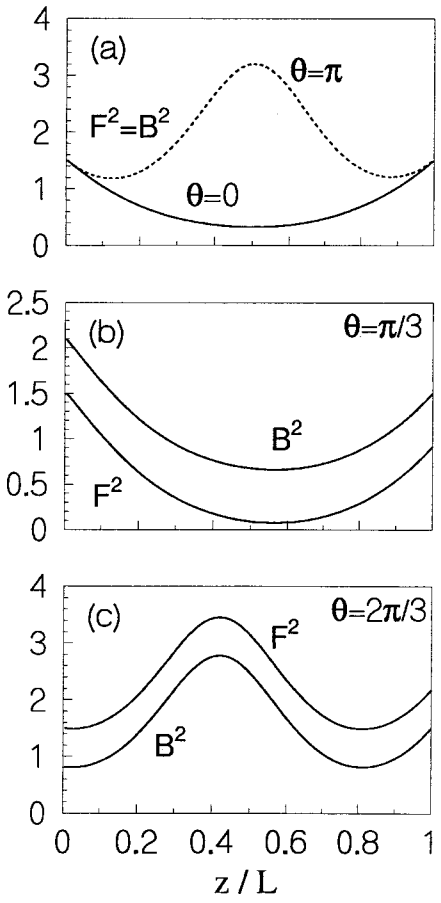

Fig. 5. (a) Two steady distributions of light intensity inside the grating at $I_0 = 1.5$; other parameters as in Fig. 2. Solid (dashed) curves correspond to in-phase (out-of-phase) incident waves. (b), (c) Other intensity distributions for θ.

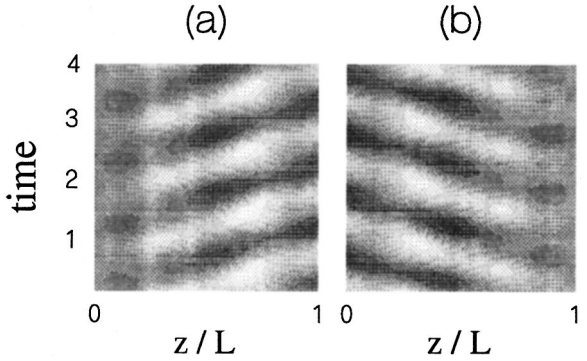

Fig. 6. Spatiotemporal patterns illustrating pulsations for (a) forward and (b) backward waves at $I_0 = 3$ and $\theta = 0$. Time is scaled in units of $t_d = Ln_0/c$. Dark (light) color corresponds to low (high) level of intensity.

Fig. 5(a). Thus a change of phase θ from zero to π leads to the appearance of a localized excitation (gap solition) in the structure.

We investigated the stability of the steady states by means of numerical simulations of the initial system of equations (1) and (2). It is known from previous studies of the NBG response to one-directional illumination that, above a certain threshold, the response becomes nonstationary.[10–12] We found that the emergence of pulsations depends on the phase difference θ. In particular, for $\theta = 0$ the lowest branch of the characteristic in Fig. 4(a) up to $I_0 = F_0^2 = B_0^2 \approx 2.8$ is stable, and pulsations arise on the upper branch of the first bistable loop. In Fig. 6 we present a space–time pattern that illustrates the formation of pulsations for forward and backward waves in the grating at $I_0 \approx 3$. It can be seen that, while the incident fields are in phase, the intensity pulsations for the fields going out from the opposite sides are out of phase [cf. the right edge of Fig. 6(a) and the left edge of Fig. 6(b)].

At $\theta = \pi$ the lower and the upper branches of the first bistable loop are stable against pulsations, and pulsations develop after the second switching at $I_0 \approx 4.3$. It should be noted that output forward and backward pulsations at $\theta = \pi$ coincide in both phase and amplitude. The spatiotemporal picture can be understood from Fig. 6, with the only difference that the pattern in Fig. 6(b) should be shifted by half of its temporal period. Thus by comparing cases $\theta = 0$ and $\theta = \pi$ one can deduce that the grating acts as a converter of a special kind: It transforms the phase of the incident field into the phase that pertains to the oscillations of the output intensity.

Studying the response of the grating for $\theta = \pi$, we also found symmetry-breaking instability. With increasing incident intensity we observed that symmetrical pulsations become nonsymmetrical for opposite directions above a certain threshold ($I_0 \gtrsim 6.5$ in terms of Fig. 4). This symmetry-breaking instability is illustrated in Fig. 7. Figure 7(a) presents output pulsations that coincide for both direction at $I_0 = 6.4$, which are transformed into nonsymmetrical pulsations at $I_0 = 6.8$ [solid and dashed

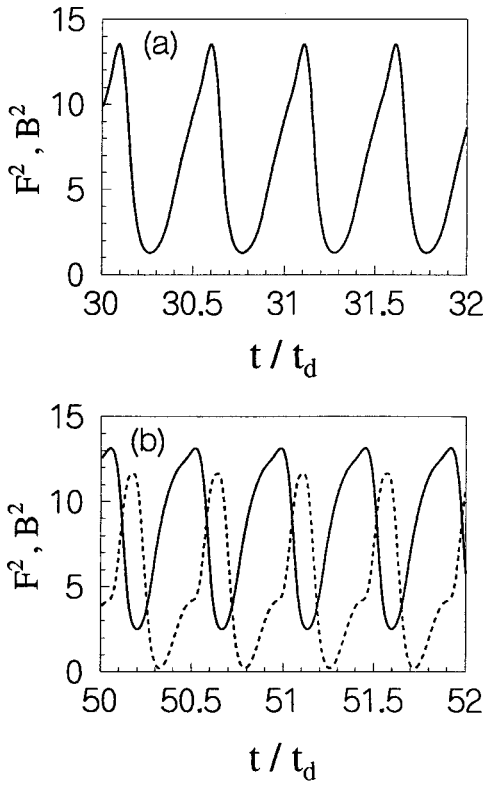

Fig. 7. Illustration of the symmetry-breaking instability at $\theta = \pi$. (a) Symmetrical output pulsations ($F^2 - B^2$) at $I_0 = 6.4$. (b) Nonsymmetrical pulsations at $I_0 = 6.8$.

curves in Fig. 7(b)]. These symmetry-breaking pulsations supplement the static symmetry-breaking bifurcation found recently in nonlinear distributed-feedback systems.[26–28]

All solutions of Eqs. (1) and (2) presented above describe the case of focusing nonlinearity ($\gamma L = 2/3$). However, by analyzing the solutions for the focusing and defocusing nonlinearities at in-phase and out-of-phase incident waves, one can note the following relationship: At $\gamma L = -2/3$ (defocusing nonlinearity), the curves in Figs. 4 and 5 remain valid, but parameter θ is changed by π. That is, the dashed curves in Figs. 4 and 5(a) correspond to in-phase incident waves, and the solid curves correspond to out-of-phase incident waves. [The only difference is that the sign of the integral C_2 presented in Fig. 4(b) should be reversed.]

It is especially easy is to analyze point ($I_0 = 1, I = 1$) in Fig. 4(a), which lies upon the unstable branch with negative slope and corresponds to the intensity constant along the grating. One can see from Eqs. (1) and (2) that at the vanishing left-hand sides the solution $E_F = 1$, $E_B = -1$ for $\gamma L = 2/3$ is transformed into the solution $E_F = 1$, $E_B = 1$ for $\gamma L = -2/3$ ($\kappa L = 2$). Note that the circumstance that this soliton lies upon the negative unstable branch may be relevant for studies in which bright or dark solitons are sought on a nonzero constant background (see, e.g., Ref. 16).

5. TRANSVERSE EFFECTS

In what follows we are dealing with spatial transverse instabilities in the NBG. This issue has no direct connection with the above-mentioned experiments with fibers, but it may be of importance for transverse effects in other wide-aperture passive and active distributed-feedback structures.[29,30] The formation of transverse spatial patterns has been rather well studied for Kerr nonlinearity without distributed feedback (see, e.g., Ref. 20), where the phases of the incident waves are not of importance. As we shall see below, for a NBG the phase parameter critically influences the threshold of the transverse instabilities as a kind of pattern emerges.

We study spatial transverse effects in the paraxial approximation, so the previous equations (1) and (2) should be complemented by the diffraction terms

$$\frac{\partial E_F}{\partial z} + \frac{n_0}{c}\frac{\partial E_F}{\partial t} = i\frac{1}{2k}\Delta_\perp E_F + i\kappa E_B \exp(-i2\delta z) + i\gamma(|E_F|^2 + 2|E_B|^2)E_F, \quad (9)$$

$$\frac{\partial E_B}{\partial z} - \frac{n_0}{c}\frac{\partial E_B}{\partial t} = -i\frac{1}{2k}\Delta_\perp E_B - i\kappa E_F \exp(i2\delta z) - i\gamma(|E_B|^2 + 2|E_F|^2)E_B, \quad (10)$$

where k is the number of light waves in the medium and $\Delta_\perp$ is a Laplacian with respect to the transverse coordinates.

We chose the size of the spatial transverse grid in our simulations by taking into account the fact that the parameter $k^2_{\text{trans}}L/k$ that characterizes the size of transverse structures $2\pi/k_{\text{trans}}$ to be formed lies between zero and 2π.[20] Typically 100 grid points for the lateral direction and 64 grid points for the transverse direction have been used. Periodic boundary conditions have been assumed, and a fast Fourier transform has been used to handle the diffraction operator. To avoid exhausting simulations we have taken only one transverse degree of freedom.

We numerically investigated transverse pattern formation in the NBG for the parameters of Fig. 4. For focusing nonlinearity at $\theta = 0$, we observed formation of static patterns above some threshold ($I_0 \approx 1.4$). A three-dimensional graph of the pattern for the forward beam obtained at $I_0 = 1.5$ is presented in Fig. 8. Similar to the behavior of the solid curve in Fig. 4(a), the light intensity decays from the edge down the structure; however, with

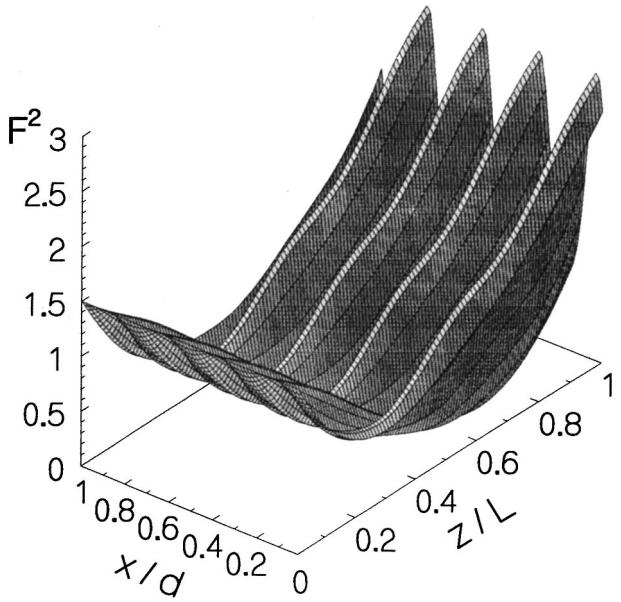

Fig. 8. Static pattern showing the forward wave intensity distribution inside the grating for the parameters of Fig. 4 and $I_F = I_B = 1.5$, $\theta = 0$, $d = 6L/k$.

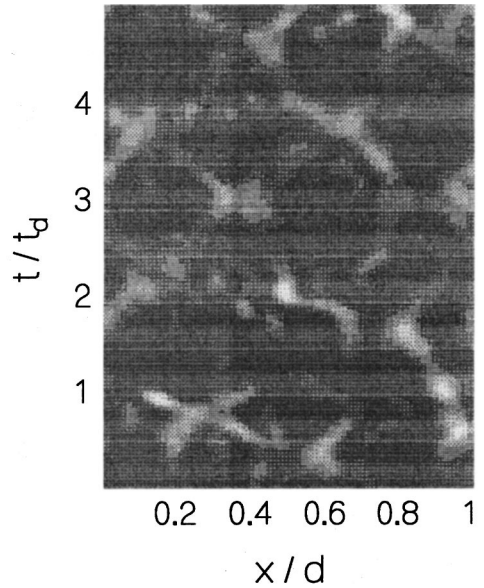

Fig. 9. (a) Space–time plot characterizing turbulent distribution of the transmitted light intensity for the parameters of Fig. 8; the only difference is that here $\theta = \pi$.

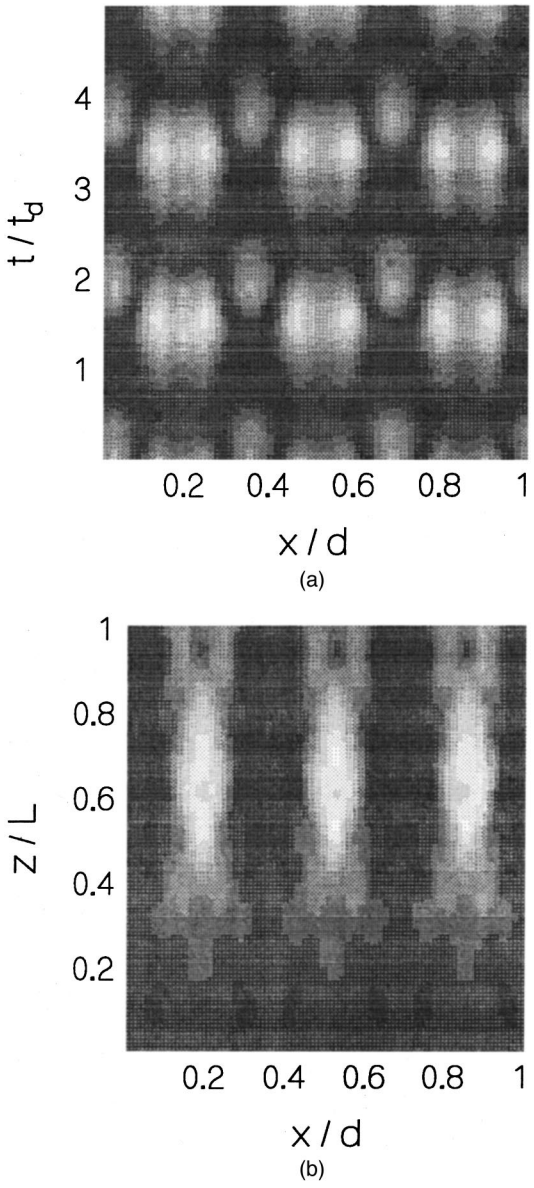

Fig. 10. (a) Space–time plot characterizing transverse distribution of the forward wave intensity at $z = L$ and $I_F = I_B = 1.5$, $\theta = \pi$, $d = 6L/k$, $\gamma L = -2/3$ (defocusing nonlinearity). Other parameters as in Fig. 4. (b) Snapshot of the pattern of light intensity inside the grating for the instant of time corresponding to the upper edge of the picture in (a).

increasing z the intensity distribution becomes increasingly more modulated in the transverse plane, and bright filaments are developed close to the back edge. The backward wave proves to be symmetric with the forward one under reflection in the plane $z = L/2$; i.e., $E_F(z, x) = E_B(L - z, x)$.

When we changed the phase difference θ by π we observed that the static pattern shown in Fig. 8 became unstable and evolved toward spatiotemporal turbulence. A space–time plot of the forward wave intensity at the back edge of the grating is shown in Fig. 9. This regime is characterized by formation of irregular spikes of the intensity inside the grating, which change their form with propagation. Symmetry for forward and backward waves is destroyed in this case, so nonreciprocal chaotic patterns are formed for waves that go out from opposite sides of the grating.

Thus the solutions that are found to be stable against temporal pulsations at $I_0 = 1.5$ when transverse effects are ignored [see the curves in Fig. 5(a)] are unstable against transverse spatiotemporal instabilities.

In the case of the defocusing nonlinearity for the same value of incident intensity $I_0 = 1.5$ and $\theta = 0$ the system is stable against transverse pattern formation. But for $\theta = \pi$ we observed formation of the regular spatiotemporal structure illustrated in Fig. 10. In Fig. 10(a) a space–time plot of the intensity of the forward wave at $z = L$ and in Fig. 10(b) a snapshot of the intensity distribution inside the grating for the instance of time corresponding to the upper edge of Fig. 10(a) are presented. One can see that a pulsated transverse pattern with a period of pulsations of nearly $2t_d$ is formed. We can see that the same transverse interval now contains three spatial periods instead of the four in Fig. 8.

With reference to the pattern in Fig. 10(a) one can say that it is similar to the structures produced by the resonant interaction between the basic transverse mode and its spatial harmonic that has a temporal (Ikeda–Hopf) component. Such structures were recently found to emerge spontaneously in passive optical systems with wide-aperture feedback[31,32] as well in pattern-forming systems of another nature, e.g., in simulations of chemical patterns.[33] One can see from the snapshot in Fig. 10(b) that (as in Fig. 8) the intensity filaments become pronounced close to the middle of the grating and then move to the back edge. The picture for the backward wave is symmetrical, with the only difference that transverse distribution of the intensity is shifted by half of a transverse structure spatial period; i.e., $E_F(z, x) = E_B(L - z, x + T_x/2)$, where T_x is the spatial period of a transverse pattern. Thus the transverse patterns for the forward and backward waves prove to be out of phase now, in contrast to the in-phase patterns obtained for focusing nonlinearity.

Note that pulsed patterns similar to those presented in Fig. 10 have been observed in our simulations for the case of unidirectional illumination on the high-transmittivity branch.

6. CONCLUSIONS

Considering the problem of interaction of light with a NBG under bidirectional illumination, we have found that the phase difference between the fields incident upon the NBG from opposite sides significantly influences the thresholds for bistability, self-pulsation, and transverse instability. Compared with that for unidirectional illumination, the threshold for bistability can be either increased or decreased, depending on the phase of the incident waves. At the out-of-phase incident fields the nonlinear Bragg structure seems to accumulate light energy more readily, which reinforces the action of nonlinearity and reduces the threshold for bistability. In turn, self-pulsations develop at lower intensities in the case of in-phase incident fields. Our calculations have been made for the parameters achievable for several solid-state

nonlinear materials. In particular, the results presented here can be verified experimentally with the help of the fiber Bragg grating used for observation of quasi-cw switching and multiple gap-soliton formation under unidirectional illumination.[3]

Our numerical simulations have shown that solutions that are stable to pulsation when transverse effects are ignored may be destabilized by means of transverse spatiotemporal instabilities. For a NBG with defocusing nonlinearity, a spatiotemporal pattern with regular dynamics may arise because of the change in the incident wave phase, whereas for focusing nonlinearity the change in the phase may cause the static pattern to become turbulent.

REFERENCES

1. B. J. Eggleton, R. E. Slusher, C. M. de Sterke, P. A. Krug, and J. E. Sipe, "Bragg grating solitons," Phys. Rev. Lett. **76**, 1627–1630 (1996).
2. B. J. Eggleton, C. M. de Sterke, and R. E. Slusher, "Nonlinear pulse propagation in Bragg gratings," J. Opt. Soc. Am. B **14**, 2980–2993 (1997).
3. D. Taverner, N. G. R. Broderick, D. J. Richardson, R. I. Laming, and M. Ibsen, "Nonlinear self-switching and multiple gap-soliton formation in a fiber Bragg grating," Opt. Lett. **23**, 328–330 (1998).
4. D. Taverner, N. G. R. Broderick, D. J. Richardson, M. Ibsen, and R. I. Laming, "All-optical AND gate based on coupled gap-soliton formation in a fiber Bragg grating," Opt. Lett. **23**, 259–261 (1998).
5. D. Campi, C. Coriasso, A. Stano, L. Faustini, C. Cacciatore, C. Rigo, and G. Meneghini, "Nonlinear contradirectional coupler," Appl. Phys. Lett. **72**, 537–539 (1998).
6. N. D. Sankey, D. F. Prelewitz, and T. G. Brown, "All-optical switching in a nonlinear periodic structures," Appl. Phys. Lett. **60**, 1427–1429 (1992).
7. C. J. Herbert and M. S. Malcuit, "Optical bistability in nonlinear periodic structures," Opt. Lett. **18**, 1783–1785 (1993).
8. J. He, M. Cada, M.-A. Dupertuis, D. Martin, F. Morier-Genoud, C. Rolland, and A. J. Springthorpe, "All-optical bistable switching and signal regeneration in a semiconductor layered distributed-feedback/Fabry–Perot structure," Appl. Phys. Lett. **63**, 866–868 (1993).
9. H. G. Winful, J. H. Marburger, and E. Garmire, "Theory of bistability in nonlinear distributed feedback structures," Appl. Phys. Lett. **35**, 379–381 (1979).
10. H. G. Winful and G. D. Cooperman, "Self-pulsing and chaos in distributed feedback bistable optical devices," Appl. Phys. Lett. **40**, 298–300 (1982).
11. H. G. Winful, R. Zamir, and S. Feldman, "Modulation instability in nonlinear periodic structures: implications for 'gap solitons,' " Appl. Phys. Lett. **58**, 1001–1003 (1991).
12. C. M. de Sterke and J. E. Sipe, "Switching dynamics of finite periodic nonlinear media: a numeric study," Phys. Rev. A **42**, 2858–2869 (1990).
13. W. Chen and D. L. Mills, "Gap solitons and the nonlinear optical response of superlattices," Phys. Rev. Lett. **58**, 160–163 (1987).
14. D. N. Christodoulides and R. I. Joseph, "Slow Bragg solitons in nonlinear periodic structures," Phys. Rev. Lett. **62**, 1746–1749 (1989).
15. A. B. Aceves and S. Wabnitz, "Self-induced transparency solitons in nonlinear refractive periodic media," Phys. Lett. A **141**, 37–42 (1989).
16. J. Feng and F. K. Kneubühl, "Solitons in a periodic structure with Kerr nonlinearity," IEEE J. Quantum Electron. **29**, 590–597 (1993).
17. C. M. de Sterke and J. E. Sipe, in *Progress in Optics*, E. Wolf, ed. (Elsevier, Amsterdam, 1994), Vol. XXXIII, p. 203.
18. S. Radic, N. Georges, and G. P. Agrawal, "Analysis of nonuniform nonlinear distributed feedback structures: generalized transfer matrix method," IEEE J. Quantum Electron. **31**, 1326–1336 (1995).
19. C. Conti, S. Trillo, and G. Assanto, "Trapping of slowly moving or stationary two-color gap solitons," Opt. Lett. **23**, 334–336 (1998).
20. J. B. Geddes, R. A. Indik, J. V. Moloney, and W. J. Firth, "Hexagons and squares in a passive nonlinear optical system," Phys. Rev. A **50**, 3471–3485 (1994).
21. H. Kogelnik and C. V. Shank, "Coupled-wave theory of distributed feedback lasers," J. Appl. Phys. **43**, 2327–2335 (1972).
22. I. S. Gradstein and I. M. Ryzhik, *Tables of Integrals, Sums, Series and Products* (Nauka, Moscow, 1971).
23. M. Wegener and C. Klingshirn, "Self-oscillations of an induced absorber (CdS) in a hybrid ring resonator," Phys. Rev. A **35**, 1740–1752 (1987).
24. I. Galbraith and H. Haug, "Spatio-temporal chaos in a ring cavity," J. Opt. Soc. Am. B **4**, 1116–1123 (1987).
25. Yu. A. Logvin and A. M. Samson, "Map limit dynamics of the chain of optically bistable thin films," Opt. Commun. **96**, 107–112 (1992); Yu. A. Logvin, A. M. Samson, and V. M. Volkov, "Spatio-temporal light structures in a chain of bistable two-level medium thin films," Solitons Chaos Fractals **4**, 1451–1460 (1994).
26. T. Peschel, U. Peschel, and F. Lederer, "Bistability and symmetry breaking in distributed coupling of counterpropagating beams into nonlinear waveguides," Phys. Rev. A **50**, 5153–5163 (1994).
27. I. V. Babushkin, Yu. A. Logvin, and N. A. Loiko, "Symmetry breaking bifurcation in light dynamics of two bistable thin films," Kvantovaya Elekron. (Moscow) **25**, 110–115 (1998) [Quantum Electron. **28**, 105–109 (1998)].
28. Yu. A. Logvin, "Nonreciprocal optical patterns due to symmetry breaking," Phys. Rev. A **57**, 1219–1222 (1998).
29. J. Zhon, M. Cada, J. He, and T. Makino, "Analysis and design of combined distributed feedback/Fabry Perot structures for surface emitting semiconductor lasers," IEEE J. Quantum Electron. **32**, 417–423 (1996).
30. A. A. Afanas'ev, V. M. Volkov, and T. S. Efendiev, "Spectrum of the transverse modes of a laser with static distributed feedback by a phase grating," Kvantovaya Elektron. (Moscow) **24**, 528–530 (1997) [Quantum Electron. **27**, 514–516 (1997)].
31. Yu. A. Logvin, B. A. Samson, A. A. Afanas'ev, A. M. Samson, and N. A. Loiko, "Triadic Hopf-static structures in two-dimensional optical pattern formation," Phys. Rev. E **54**, R4548–R4551 (1996).
32. Yu. A. Logvin, T. Ackemann, and W. Lange, "Winking hexagons," Europhys. Lett. **38**, 583–588 (1997).
33. A. De Wit, D. Lima, G. Dewel, and P. Borckmans, "Spatiotemporal dynamics near a codimension-two point," Phys. Rev. E **54**, 261–271 (1996).